Study and optimization of boronization in Alcator C-Mod using the Surface Science Station (S[superscript 3])

Citation: Ochoukov, Roman, Dennis Whyte, Bruce Lipschultz, Brian LaBombard, Niels Gierse, and Soren Harrison. "Study and Optimization of Boronization in Alcator C-Mod Using the Surface Science Station (S[superscript 3])." Fusion Engineering and Design 87, no. 9 (September 2012): 1700–1707.

As Published: http://dx.doi.org/10.1016/j.fusengdes.2012.07.013

Publisher: Elsevier

Persistent URL: http://hdl.handle.net/1721.1/99454

Version: Author's final manuscript: final author's manuscript post peer review, without publisher's formatting or copy editing

PSFC/JA-12-25

Study and Optimization of Boronization in Alcator C-Mod using the Surface Science Station (S^3)

Ochoukov, R., Whyte, D.G., Lipschultz, B., LaBombard, B., Gierse, N.[*], and Harrison, S.[**]

**Institute of Energy and Climate Research - Plasma Physics, Forschungszentrum Jülich GmbH, Association EURATOM-FZJ, Partner in the Trilateral Euregio Cluster, Jülich, Germany* and
I. Physikalisches Institut, Universität zu Köln, D-50937 Cologne, Germany.
***Fusion Research Technologies, 519 Somerville Avenue #243, Somerville, MA 02143*.

July, 2012

Plasma Science and Fusion Center
Massachusetts Institute of Technology
Cambridge MA 02139 USA

This work was supported by the U.S. Department of Energy, Grant No. DE-FC02-99ER54512. Reproduction, translation, publication, use and disposal, in whole or in part, by or for the United States government is permitted.
Submitted for publication to journal of *Fusion Engineering and Design*.

Study and Optimization of Boronization in Alcator C-Mod using the Surface Science Station (S^3)

Roman Ochoukov[a*], Dennis Whyte[a], Bruce Lipschultz[a], Brian LaBombard[a], Niels Gierse[b], and Soren Harrison[c]

[a]*Plasma Science and Fusion Center MIT, NW17, 175 Albany Street, Cambridge, MA, 02139, USA.*

[b]*Institute of Energy and Climate Research - Plasma Physics, Forschungszentrum Jülich GmbH, Association EURATOM-FZJ, Partner in the Trilateral Euregio Cluster, Jülich, Germany* and *I. Physikalisches Institut, Universität zu Köln, D-50937 Cologne, Germany.*

[c]*Fusion Research Technologies, 519 Somerville Avenue #243, Somerville, MA 02143.*

[*]*Corresponding author address:* 175 Albany St., Cambridge, MA, 02139, USA.

[*]*Corresponding author:* Roman Ochoukov, ochoukov@psfc.mit.edu, 617-253-5395.

Abstract

A Surface Science Station (S^3) on the Alcator C-Mod tokamak is used to study and optimize the location and rate of boron film deposition *in-situ* during electron cyclotron (EC) discharge plasmas using 2.45 GHz radio-frequency (RF) heating and a mixture of helium and diborane (B_2D_6) gasses. The radial profile of boron deposition is measured with a pair of quartz microbalances (QMB) on S^3, the faces of which can be rotated 360^o including orientations parallel and perpendicular to the toroidal magnetic field B_T ~0.1 T. The plasma electron density is measured with a Langmuir probe, also on S^3 in the vicinity of the QMBs, and typical values are ~1x10^{16} m^{-3}. A maximum boron deposition rate of 0.82 μg/cm^2/min is obtained, which corresponds to 3.5 nm/min if the film density is that of solid boron. These deposition rates are sufficient for boron film applications between tokamak discharges. However the deposition does not peak at the EC resonance as previously assumed. Rather, deposition peaks near the upper hybrid (UH) resonance, ~5 cm outboard of the EC resonance. This has implications for RF absorption, with the RF waves being no longer damped on the electrons at the EC resonance. The previously inferred radial locations of critical erosion zones in Alcator C-Mod also need to be re-evaluated. The boron deposition profile versus major radius follows the ion flux/density profile, implying that the boron deposition is primarily ionic. The application of a vertical magnetic field (B_V ~0.01 T) was found to narrow the plasma density and boron deposition profiles near the UH resonance, thus better localizing the deposition. A Monte Carlo simulation is developed to model the boron deposition on the different QMB/tokamak surfaces. The model requires a relatively high boron ion gyroradius of ~5 mm, indicating a B^{+1} ion temperature of ~2 eV, to match the deposition on QMB surfaces with different orientation to B_T. Additionally, the boron ion trajectories become de-magnetized at high neutral gas throughput (~0.5 Pa m^3 s^{-1}) and pressure (~2 Pa) when the largest absolute deposition rates are measured, resulting in deposition patterns, which are independent of surface orientation to B_T in optimized conditions.

Keywords: Alcator C-Mod; boronization; quartz microbalance; Monte Carlo simulation.

Abbreviations

S^3 – Surface Science Station
EC – electron cyclotron
RF – radio frequency
QMB – quartz microbalance
UH – upper hybrid
PFC – plasma facing component
ICRF – ion cyclotron resonance frequency
ECDC – electron cyclotron discharge cleaning

1. Introduction

The Alcator C-Mod tokamak is a fusion experiment that uses only high-Z refractory metal, molybdenum (Mo) and tungsten (W), as plasma facing components (PFCs) [1]. Although tungsten is favored for PFC applications in nuclear fusion reactors due to its resistance to neutron damage, low tritium retention, low erosion yield, and high resistance to thermal fluxes, it has a significant drawback; the plasma tolerance to high-Z impurities is low and a small fraction ($n_W/n_e \geq 10^{-5}$-10^{-4}) of Mo or W in the plasma leads to high core line radiation losses, resulting in poor fusion performance. The detrimental effects of high-Z impurities in present fusion devices are well documented. In particular C-Mod finds high core Mo fractions and accompanying radiation in ion cyclotron resonance frequency (ICRF) heated H-modes [2-4]. The problem of ICRF-enhanced erosion of high-Z materials is also documented in ASDEX-Upgrade with W-coated PFCs [5].

Previous Alcator C-Mod experiments were aimed at understanding and minimizing the role of ICRF in enhancing Mo erosion and core contamination [2-3]. An important research and operational strategy in these efforts is to reduce the surface area of Mo exposed to the plasma in order to infer important locations of Mo erosion. However it is impractical to change the actual PFCs since this requires entrance into the vacuum vessel. Rather, this is accomplished by coating the molybdenum PFCs with a thin layer (< micron) of a low-Z material, boron (B). The process of depositing such layers of B is traditionally called 'boronization' [6, 7]. There are several techniques to deposit boron films on the PFCs: a glow discharge plasma used on TEXTOR [7] DIII-D [8], and MAST [9], an electron cyclotron discharge (ECD) plasma used on Alcator C-Mod [3], or an ion cyclotron discharge (ICD) plasma used on EAST [10]. The C-Mod boronizations utilize an ECD plasma. The ECD technique relies on the fact that the vacuum toroidal magnetic field (B_T), and hence the electron cyclotron frequency, is inversely proportional to the major radius (R): if a radio-frequency (RF) wave of a fixed frequency is injected into the device from the low-field side then the wave is absorbed at the R location where the wave frequency becomes equal to the EC frequency. The location of the absorption can be swept in R by changing the magnitude of the on-axis toroidal magnetic field. The specifics of the ECD procedure employed on the Alcator C-Mod tokamak will be described in detail in Section 2.

By covering the Mo surfaces, boronization has been shown to be successful at strongly reducing the core Mo content, and associated detrimental effects, such that high-quality H-modes were possible [2]. However these positive effects are short-lived: after 20-40 ICRF-heated discharges (~1-2 s duration each) following a boronization the core Mo level increased to unacceptable levels, caused by the removal of the B film exposing the Mo underneath. These studies inferred that the deposited boron films are removed non-uniformly from the vessel's plasma facing materials [2, 3, 11]: the fastest boron erosion appeared to occur at the major radius location corresponding to the horizontal outer divertor shelf and the limiters. This localization was deduced from the longevity of Mo suppression versus the EC resonance location, R_{EC}, used

during boronization. It was assumed that B deposition would peak at the EC resonance. However no direct diagnosis of the boron film thickness and location from the boronization was available. This caused uncertainty in the inferred net erosion rates of B and the critical locations of Mo sources in C-Mod.

The goals of this study are to characterize and optimize the boronization procedure on the Alcator C-Mod tokamak. Some of the motivating questions are:
(1) What exactly is the boron spatial deposition pattern and what does it tell us about inferred erosion locations for B and Mo [3]? (2) What controls the pattern of deposition on various surfaces? (3) *Does the orientation of the PFC surface with respect to the applied magnetic field play a role in the boron deposition; for example, toroidally localized limiters vs. divertor surfaces?* (4) *Is it possible to improve the localization of the boron deposition profile in the locations where boron and molybdenum erosion is critical?* This localization is also desirable to decrease unwanted B deposition near the ICRF antenna surfaces (R ~0.90-0.95 m): these surfaces require additional conditioning, before normal ICRF operation is recovered. It is also worth noting that ECDC is a wall conditioning technique that can be applied in long pulse devices with permanently energized superconducting toroidal field magnets, such as ITER. Therefore, the benefits of optimizing ECDC wall conditioning may extend beyond Alcator C-Mod to future long pulse tokamaks.

2. Experimental Apparatus and Procedure

Alcator C-Mod is a high field ($B_T \leq 9$ T) compact (major radius $R_o = 0.67$ m, minor radius a = 0.2 m) divertor tokamak [1]. The boronization of Alcator C-Mod is performed using a helium-diborane gas mixture (10-20% B_2D_6, 80-90% He) in an ECD plasma. The gas mixture is injected from a toroidally-axisymmetric pipe located at the top of the vessel. The pipe contains a series of holes ~1 cm apart toroidally to ensure that the diborane mixture is injected uniformly toroidally throughout the vessel. The plasma is created by launching electromagnetic waves at a fixed frequency ($f_{RF} = 2.45$ GHz) and power (~3 kW) from a horn located at a single outboard toroidal location (J-Port [4]). Throughout the boronization the toroidal field magnets remain energized and create a steady-state toroidal field ($0.059 \leq B_T \leq 0.13$ T on axis). The RF waves are resonant with the electron cyclotron frequency at a major radius (R_{EC}, [m]) of:

$$R_{EC} = \frac{q_e B_T R_o}{2\pi m_e f_{RF}}, \qquad \text{Eq. (2.1)}$$

where q_e is the electron charge in C and m_e is the electron mass in kg. For the case of Alcator C-Mod, this equation simplifies to R_{EC} [m] = 7.64 B_T, where B_T in tesla. By changing B_T, R_{EC} can be swept over the radial extent of the C-Mod vacuum vessel (R=0.5-1.1 m). Equilibrium field coils can be used to apply a steady-state vertical magnetic field ($B_V \sim 0.1 B_T$).

Deuterium-only (D_2) ECD plasma discharges in Alcator C-Mod have been previously studied by Nachtrieb et al. [12] using an omegatron Z/M spectrometer, a retarding field ion energy analyzer, and Langmuir probes. Neutral in-vessel gas pressure ranged between $0.133 \leq P_{in\text{-}vessel} \leq 2.67$ Pa. Nachtrieb showed that the electron density (n_e) is on the order of 1-2x10^{16} m^{-3} at the lower neutral pressure values and decreases to <10^{16} m^{-3} at the highest neutral in-vessel pressures. Sweeping the EC resonance location past the fixed diagnostics (R = 0.74 m) show that n_e sharply drops an order of magnitude inside R_{EC} ($R < R_{EC}$), consistent with radially outward ExB polarization drift in the purely toroidal B_T field. However n_e did not peak at R_{EC}, but rather $R - R_{EC} = \Delta R \sim 0.05$ m, i.e. outboard of the EC resonance. Similarly, the D^+ ion temperature peaks at $\Delta R \sim 0.05$ m with maximum $T_i \sim 5$-10 eV, with T_i dropping sharply for $\Delta R < 0.05$ m. The electron temperature $T_e \sim 10$ eV is approximately constant versus R. As the neutral gas pressure is increased, the electron temperature remains at ~10 eV but the peak ion temperature drops to ~1-2 eV.

Note that n_e and T_i profile measurements by Nachtrieb [12] may not necessarily represent the boron deposition profile during boronization: B^+ ions are a minority species in an ECDC discharge, however, the n_e and RF wave absorption profiles are set by the main ion species (He^+ during boronization and D^+ in Nachtrieb et al. experiment [12]). Therefore, a direct measurement of boron deposition rates is needed to determine boron deposition profiles on the plasma facing components during boronization of Alcator C-Mod.

The recently installed Surface Science Station (S^3) is the experimental apparatus used in this study and is shown in Figure 2.1. The apparatus consists of ~2 m re-entrant tube armed with a replaceable diagnostics head. The probe enters 0.22 m below the mid-plane, and can be positioned from R=0.58 m out to its entry port at R=1.3 m which is effectively the outboard limit of the vacuum vessel. The S^3 head is also capable of rotating about its insertion axis by ± 90°. The system allows retraction of the diagnostic head behind a vacuum gate valve for up-to-air maintenance.

The head used for these studies contained two quartz micro-balances (QMBs, the crystals and vacuum components provided by McVac Manufacturing Co. Inc., the QMB controller provided by Sigma Instruments, Model SQC-300) to measure boron deposition/erosion rates, two thermocouples attached to the QMB housing to monitor their temperatures, and a Langmuir probe to measure the ion saturation current (I_{sat}), T_e, and n_e in ECD plasmas. The orientation of the QMB faces is shown in Figure. 2.1. The "radially viewing" QMB, i.e. QMB1 with its face parallel to toroidal direction, is recessed several mm inside the head and cannot directly intercept magnetic field lines. The "poloidally and toroidally viewing" QMB, i.e. QMB2 with its face parallel to R, has variable orientation to B with the 0° position of the head defined to be the face viewing upward.

The boron film deposition on the QMB surface is estimated from the change in the resonance frequency of the QMB quartz crystals using the QCM equation [13]. The QCM equation provides the mass change per unit area ($\Delta m/A$) on the surface of the crystal. However, assuming that the density of the deposited film is that of solid boron ($n_B = 1.30 \times 10^{29}$ m^{-3} or 2.37 g/cm^3) allows us to estimate the boron film deposition thickness (Δd). Our density assumption is not unreasonable, considering typical density values for carbon-based co-deposits of 0.9-2.4 g/cm^3 [14]. Our value is also within a factor 0.7 from the density value of 1.6 g/cm^3 used to estimate co-deposit thicknesses on QMBs in NSTX [15]. Since the resonance frequency change of the crystals during boron deposition (Δf [Hz]) is at least 1,000 times smaller than the value of the resonance frequency ($f_C \sim 6 \times 10^6$ Hz), we may approximate the QCM equation as:

$$\Delta m/A \ [\mu g/cm^2] = 0.012 \Delta f \ [Hz], \qquad \text{Eq. (2.2)}$$

or, using the solid boron density assumption:

$$\Delta d \ [nm] = 0.052 \Delta f \ [Hz], \qquad \text{Eq. (2.3)}$$

The temperature of the QMB surfaces was kept constant to within ±0.02 °C for these experiments by active cooling with N_2 gas in order to minimize thermal-induced drifting of the crystal's resonant frequency. The absolute temperature of the QMB housing ranged between 30-33 °C depending on the experimental conditions.

In-vessel neutral gas pressure was measured with a baratron capacitance pressure gauge [12]. The gas/particle throughput during boronization is obtained from the foreline pressure ($P_{foreline}$) at

the vacuum pump's inlet, assuming that the pumping speed remains constant (0.017 m^3 s^{-1} per pump) over the pressure range ($4.0 < P_{foreline} < 14.7$ Pa) of these experiments.

To obtain the radial boron deposition rate profile, the S^3 head was scanned along R in steps of 0.05 or 0.1 m. At each step the QMB is sampled over a 30-60 s time interval with the time resolution of ~1.5 s. The QMB temperature and the neutral in-vessel gas pressure were monitored with the same time resolution. A "snap shot" of QMB data is shown in Figure 2.2; S^3 position $R_{probe} = 0.75$ m, $R_{EC} = 0.60$ m, QMB2 orientation $\theta = 90^o$ (i.e. facing into B-field). The plot shows an approximately linearly decreasing resonant frequency of the QMBs. Linear fits to the frequency and application of Eq. 2 (or Eq. 3) provide boron deposition rates of 0.18 and 0.20 $\mu g/cm^2$/min (or 0.74 and 0.83 nm/min) for QMB1 and QMB2 respectively in this case.

3. Experimental Results

The ECD plasma density profile depends on several key experimental parameters such as the EC resonance location, vertical magnetic field, gas mixture and particle throughput. The effect of these parameters on the radial plasma density profiles is shown in Figure. 3.1. Here, an assumption is made that the plasma density profile follows the ion saturation current profile. This assumption is valid as long as the electron temperature and the probe collection area remain constant. A typical ECD discharge on Alcator C-Mod meets these criteria with T_e ~constant = 10 eV across the plasma profile [12].

Both the presence of diborane and the neutral density affect the shape and magnitude of the radial density profile (Figure. 3.1). Two in-vessel pressures (mid-range: 0.7 Pa, high-range: 2 Pa) are examined, corresponding to boron particle throughputs of 0.062 and 0.080 Pa m^3 s^{-1} respectively (or, equivalently, 1.5×10^{19} and 1.9×10^{19} B/s at 10% diborane mixture). In all He-only cases the I_{sat} and, hence, n_e decreases at the higher pressure (in agreement with D_2-only results of [12]), suggesting that at fixed RF power the plasma is ionization limited. Yet this trend is reversed with the 10% diborane mixture, suggesting that even at 10% the diborane has a significant effect on particle balance due to its lower ionization threshold.

A notable feature appearing on the profiles is that in all cases (Figure. 3.1) the peak in I_{sat} is outboard from the EC resonance, which is attributed to ionization at the upper hybrid (UH) resonance. From the definition of the upper hybrid frequency, f_{UH}, [16]:

$$f_{UH}[Hz] = \frac{1}{2\pi}\left(\frac{n_e q_e^{\,2}}{\varepsilon_o m_e} + \frac{q_e^{\,2} B_T^{\,2}}{m_e^{\,2}}\right)^{1/2} \quad \text{, Eq. (3.1)}$$

where ε_o is the vacuum permittivity. Substituting $B = B_o R_o / R$ we can estimate the radial location of the upper hybrid resonance, R_{UH}, in Alcator C-Mod ECDC plasmas as:

$$R_{UH}[m] = R_{EC}\left(1 - 0.134\frac{n_e}{10^{16}}\right)^{-1/2} \quad \text{, Eq. (3.2)}$$

which typically results in the UH resonance being located 0.04-0.06 m outboard of R_{EC} (hatched region of Figure. 3.1). This suggests that the EC resonance is not the dominant absorption location for RF power [12]. Nachtrieb et al [12] also observed the density and T_i peak shifted from the EC resonance location, suggesting that ion heating occurs at the UH location. The density decreases rapidly for $R > R_{LIMITER} = 0.82$ m due to sudden shortening of the parallel connection length, $L_{//}$, due to the limiter.

Applying a vertical magnetic field (B_V/B_T ~0.1) affects the n_e radial profile (note that previous ECD study results [12] were obtained with $B_V = 0$ T). The purpose of the vertical magnetic field component is to set a finite $L_{//}$ at $R < R_{limiter}$, i.e. field lines now terminate on the top and bottom

divertor structures. As a result, the plasma transport and loss along the field lines begins to compete with the cross-field transport due to the ∇B drift to better concentrate ion flux to the divertors. From Figure 3.1 it can be seen that the vertical magnetic field is effective at peaking the I_{sat} near R_{UH} in the presence of diborane: the peak I_{sat} value increases with the vertical field and the effect is more pronounced at the higher particle throughput.

Pressure and vertical field affect the plasma profiles and deposition rates. Figure 3.2 shows the radial profiles of boron deposition rate at the approximate mid-range of in-vessel pressure (corresponding to a 0.062 Pa m^3 s^{-1} or $1.5x10^{19}$ boron atoms/s throughput) on the QMB surfaces oriented parallel (//) and perpendicular (⊥) to the magnetic field. The boron deposition profiles generally follow the plasma density profiles and are similarly peaked near the UH resonance. The general correlation between the I_{sat} and boron deposition rate profiles indicates that the deposition is mainly ionic. The low fraction of net boron deposition occurring in the neutral state is confirmed by a very low boron deposition rate (~$7x10^{-4}$ μg/cm^2/min or ~0.003 nm/min) when the QMBs in the diagnostic head are retracted into the shelter of the entrance port with R_{PROBE} = R_{PORT} = 1.3 m. The QMBs are thus shielded from the plasma and the deposition can only be due to neutral boron atoms. Assuming that neutral boron atoms are created on a cylindrical surface defined by R = $R_{EC/UH}$ implies that the neutral boron flux follows the 1/R dependence for R > $R_{EC/UH}$. Extrapolating the measured deposition rate inward to R = 0.7 m gives an expected neutral-only deposition rate ~0.0014 μg/cm^2/min (or ~0.006 nm/min), much less than the measured boron deposition rates of 0.2-0.5 μg/cm^2/min (or 1-2 nm/min), verifying that deposition is primarily ionic.

Figure 3.2 also shows that the ratio of deposition between the surfaces perpendicular and parallel to the B-field is ~2. Since boron deposition is primarily ionic, the B^+ ion gyroradius (ρ_{B+}) must be large, comparable to the scale length of the QMB housing (~6 mm), in order to have significant boron deposition on the QMB surface parallel to the magnetic field. The effect of the sheath electric field on the boron ion trajectories may be ignored due to the small size (<1 mm) of the sheath thickness at the experimental plasma conditions (n_e ~$1x10^{16}$ m^{-3}, T_e ~10 eV). At the experimental ECD magnetic fields of ~0.1 T, this ion gyro radius implies B^+ ion temperature ~2 eV, i.e. well above the neutral gas temperature ~0.025 eV. That T_i is well above room temperature is consistent with independent C-Mod T_i measurements of Nachtrieb et al. [12] (~10 eV at the UH resonance) using the omegatron in a deuterium ECD plasma. Their T_i radial profile is also peaked at the UH resonance, suggesting that the RF wave absorption takes place not at the EC but at the UH location.

The total boron deposition in the vessel estimated from the radial profiles of boron deposition rate (2-4 g) is comparable to the total amount of injected boron atoms (~4 g) indicating global particle balance and accurate absolute deposition rates; see the following text for an estimate of the global boron atom balance during boronization of Alcator C-Mod. The deposition area is assumed to be washer-like, centered at R_o = 67 cm and 40 cm wide; area = $2\pi*67*40 = 1.7x10^4$

cm^2, and the density of boron is taken as 2.37 g/cm^3. Radially integrating the deposition rates of Figure 3.2, accounting for two deposition surfaces at the top and bottom of the vessel, and noting that the boronization occurs over 9.5 hrs = 570 mins, we obtain 2–4 g of boron deposited in the vessel. The lower bound is for the surface parallel to the magnetic field and the upper bound is for the surface perpendicular to the magnetic field. This compares to ~4 g of boron that flows into the machine during the boronization as estimated from the pressure change in the diborane bottle. Previous diagnosis of diborane in the ECD exhaust has found that extremely little of diborane leaves the vessel, and thus is assumed to be deposited in the device. Thus the boron deposited in C-Mod at mid-range of pressure/throughput is well accounted for, considering the variation in the deposition rates on various in-vessel surfaces.

The particle flow-through (or neutral gas pressure) utilized during boronization can also have strong effects on the boronization rate and the processes involved. Figure 3.3 (a) demonstrates that the boron deposition rate increases monotonically with boron throughput up to 0.12 Pa $m^3 s^{-1}$. The deposition rate does not appear to depend explicitly on the diborane fraction. For the 10% case the perpendicular boron deposition rate peaks at 0.59 $\mu g/cm^2$/min (or 2.5 nm/min) at 0.07 Pa m^3 s^{-1} of boron throughput. Simultaneously as the throughput increases, Figure 3.3 (b) shows that the ratio of the perpendicular to parallel deposition rates approaches unity, i.e. the boron deposition becomes independent of the surface orientation to the magnetic field. For the 20% diborane mixture case, deposition peaks at 0.71-0.83 $\mu g/cm^2$/min (or 3-3.5 nm/min), but rolls over as the throughput (pressure) is increased past 0.12 Pa m^3 s^{-1}. The ratio of perpendicular to parallel deposition at 20% mixture follows the same trend as the 10% case, i.e. decreasing with throughput, yet approaches unity at a B throughput ~ 0.15 Pa m^3 s^{-1}, about 50% higher than in the 10% case. This suggests qualitatively that the He pressure, which makes up the remainder of the in-vessel particle inventory, is also playing a role in the deposition pattern.

Simultaneously the observation that He plays a role in deposition processes raises concerns about the direct effect of He on the deposition: for example does the He participate in re-eroding the boron film? However, repeated exposures of the QMBs' with pure He plasma indicate that the helium plasma produced neither erosion nor deposition of B films to within measurement uncertainty (<0.02 $\mu g/cm^2$/min or <0.1 nm/min) for all the total particle throughput values plotted in Figure 3.3. Therefore the effect of He appears to be limited to the spatial pattern of deposition rather than some direct influence on the boron films. This effect will be further examined and modeled in Section 4.

The turnover of the boron deposition rate as the boron throughput is increased past 0.12 Pa m^3 s^{-1} (Figure 3.3 a) indicates that the ECDC discharge has become power-limited, i.e. there is insufficient RF power for ionization to keep pace with increasing neutral particle flow through (Note this does not invalidate the B particle balance described above at mid-pressure ranges). This observation is supported by simple power balance at boron throughput ~0.15 Pa m^3 s^{-1} or a total (He and B) flow through rate (I) I ~0.8 Pa m^3 s^{-1} ~$2x10^{20}$ particles/s. We roughly estimate

that each particle dissociation and/or ionization requires $E_{ionization}$~ 75-100 eV due to the fact that in low T_e plasmas there is 3-4 times ionization energy loss in radiation [17]. The implied power to supply this ionization is then k_B I $E_{ionization}$~2.4 – 3.2 kW, which is in good agreement with the total RF power supplied of 3 kW; k_B is the Boltzmann constant. The deposition rate turnover suggests that more input RF power would be needed to obtain even higher deposition rates at the boron throughput >0.12 Pa m^3 s^{-1}. This further supports the observation that ions dominate depositions rather than neutrals.

The correlation between local ion flux and boron deposition rate is shown in Figure 3.4 at a fixed "intermediate" boron throughput. Regardless of QMB orientation, the deposition rate monotonically increases with ion flux, which we attribute to the mainly ionic deposition mechanism. This correlation holds for the parallel surfaces that do not directly intercept the magnetic field lines, implying that the boron ions have sufficiently large temperature and, hence, gyroradii to intercept such surfaces. The inferred ionic fraction of boron is ~20% at low ion flux and between 5-10% at higher ion flux. These fractions are reasonable considering the 10% B_2D_6, 90% He neutral gas mixture, yet also indicates that there is some variation in the ion mixture, likely due to differences in ionization of the boron and the background helium.

The importance of applying the vertical magnetic field to increase the plasma density and hence the local boron deposition rates at the UH resonance location becomes apparent after examining Figure 3.4: the plasma density, the plasma flux, and the boron deposition rates nearly double in the presence of the vertical magnetic field. The boron deposition rate continues to increase with higher incident ion flux, imply that even higher deposition rates are attainable, provided adequate (or additional) RF power is supplied to keep up ionization.

4. Monte Carlo Numerical Simulation of Deposition Patterns

The ratio between the peak boron deposition rates measured on the QMB surfaces parallel and perpendicular to the magnetic field suggests a B^+ ion temperature of a few eV, since the corresponding ion Larmor radius needs to be large enough for the ions to reach the shielded // QMB surface. This implies that the Larmor radius (ρ_{B+}) is on the order of a few mm (e.g. ρ_{B+} = 8 mm when T_{B+} = 5 eV and B = 0.09 T). However, the geometrical dimensions of the deposition surfaces are also a few mm in diameter: the radius of the collecting QMB surface (r_{QMB}) is 3 mm and the radius of the limiter-like shielding washer around the QMB surface is 13 mm. Additionally, the ion-neutral collision mean free path between B^+ ions and He atoms (λ_{i-n}) varies over a large range in the experiment due to the large range in "background" neutral He pressure (or density). Due to this large variation in λ_{i-n} the Hall coefficient ($\beta \equiv \lambda_{i-n}/\rho_{B+}$),, which is an indicator of the boron ions trajectories' degree of magnetization, can decrease to order unity in the high $P_{neutral}$ regime. A low Hall coefficient would suggest that boron ions, on average, scatter off a neutral He atom before completing a full Larmor orbit. Therefore, one concludes that key physical dimensions (λ_{i-n}, ρ_{B+}, r_{QMB}) are of a comparable size and the problem of determining the boron deposition profiles or patterns on real surfaces should be treated numerically.

To test our hypothesis that the deposition of boron takes place in the form of B^+ ions at the boron ion temperature T_{B+} of a few eV, a Monte Carlo numerical model is developed that follows B^+ ion trajectories and deposition on arbitrary geometrical surfaces. The model's algorithm launches ions randomly with a uniform particle density in a 15x15x15 cm^3 test volume. The initial ion velocity distribution is set by T_{B+} and the ions are followed assuming collisionless or collisional (with neutral He atoms) trajectories. Ion-neutral collisions were treated as elastic "hard sphere" collisions [18]. The deposition rate was simulated by tallying all B^+ ions crossing the modeled QMB surfaces. The ∇B ion drift was included when calculating the ion trajectories.

Figure 4.1 displays the simulated boron deposition rate ratio for the two QMB faces as a function of the B^+ ion temperature. The range of expected ion temperatures is also shown by a shaded region. If the deposited boron ions were at room temperature (~0.025 eV), as initially suspected, then the expected ratio between the boron deposition on the QMB surfaces perpendicular and parallel to the magnetic field would be >>1. The small size of the thermal ion larmor radius (0.5 mm) would prevent the majority of the boron ions from reaching the QMB surface parallel to the magnetic field. The experimentally observed ratio is 1-3 and matches the numerical results for T_i ~1-10 eV. This temperature agrees well with Nachtrieb's measurements of T_i ~5-10 eV in deuterium ECD plasmas [12].

The same deposition is expected on the two QMBs when they are both oriented parallel to the magnetic field, i.e. when QMB2 surface is viewing vertically upward (0 degree orientation, Figure 2.1 (a)). At the same time, in the absence of collisions, one would expect an increasing deposition rate on QMB2 as the S^3 rotates and its surface is perpendicular to the magnetic field, which allows it to intercept directly parallel streaming boron ions. These trends are confirmed in

the experiment and model using realistic gyromotion to T_{B+} ~2 eV in Figure 4.2. The data from the S^3 probe as it is rotated under constant boronization background conditions and the ratio of the boron deposition rate between the two QMB surfaces is measured. As expected the ratio is near unity at 0 degrees since the surfaces are both parallel to the magnetic field, and the ratio increases to ~2-3 as the QMB2 face is turned into the magnetic field (the other QMB, of course, does not change its orientation to the magnetic field). This dependence on the QMB surface orientations is well reproduced in the Monte Carlo simulation, assuming the B^+ ion temperature T_{B+} = 2 eV without collisions. In this case the neutral density was low and, therefore, the ion trajectories are strongly magnetized. The fact that the ratio of deposition only increases by ~2x is a qualitative indicator that the boron ions must have gyroradii ~QMB radii in order to access the surface // to the magnetic field. This qualitative picture is confirmed by the MC orbit following with a sufficiently high ion temperature ~2 eV, well in excess of room temperature and consistent with the T_i measurements of Nachtrieb [12]. This is a further demonstration that the ions are somehow heated to substantial fraction of the electron temperature. Because this ion temperature is obtained in the absence of confinement it indicates that some RF power absorption is directly occurring onto the ions. From the point of view of boronization, this is a critical result since it indicates that even in the absence of ion-neutral collisions there will be substantial boron deposition rates on surfaces oriented // to the magnetic field as long as the local surface structure or recess is on the order of 1 cm. Therefore, we can expect a complicated pattern, for instance, on limiter sides. Increasing the neutral gas density in the ECD plasma decreases the mean free path of the ion-neutral collisions and can lead to de-magnetized boron ions in the plasma if the mean free distance is less than a gyroradius. If this happens, then one expects that the boron deposition profile becomes nearly independent of the surface orientation to the magnetic field.

Deposition rates independent of the magnetic field orientation are, in fact, observed experimentally at the highest neutral in-vessel gas pressures of ~2 Pa, corresponding to $5x10^{20}$ m^{-3} neutral He gas density as shown in Figure 4.3. The trend of uniform deposition at a gas density ~$5x10^{20}$ m^{-3} is reproduced in the numerical simulation assuming the gas is at room temperature. Note that the modeled ratio is less sensitive to neutral pressure than the experimental results and the transition to the de-magnetized regime (when $\perp$ deposition $\approx$ // deposition) occurs at lower density in the simulation. This indicates that the neutral collisional model may not be fully accurate or that the assumption of room temperature neutrals is too simplistic.

We conclude that the boron deposition has two regimes dependent on the neutral gas pressure: 1) at low $P_{neutral}$ the B^+ ion trajectories are magnetized and the finite ρ_{B+} sets the deposition profile and 2) at high $P_{neutral}$ the B^+ ion trajectories are de-magnetized and the deposition profile is independent of the surface orientation to the magnetic field. The important conclusion is that for regimes of most interest operationally for C-Mod, i.e. at the highest deposition rate, the boron

deposition can be treated as being nearly isotropic in space, which makes predicting the boron film thickness on complicated internal structures much easier.

5. Discussion & Summary

Our investigation of boronization in Alcator C-Mod established that the boron deposition process on the inner walls of the vessel is primarily ionic and its local deposition pattern is determined by the degree of magnetization of the boron ion trajectories. For the cases when the boron ion trajectories are magnetized, the deposition profile is then determined by the Larmor radius of the ions. The demagnetization of the boron ion trajectories is a result of the collisions with the neutral He atoms and becomes dominant at high neutral gas pressures / densities.

Furthermore, when ion trajectories are magnetized the B^+ gyroradius must be several mm to explain the deposition on surfaces parallel and perpendicular to the magnetic field, indicating a B^+ ion temperature of ~2 eV in a magnetic field of ~0.1 T, well in excess of room temperature. These results are also supported by a Monte Carlo simulation. Previous direct measurements of the background He ions by Nachtrieb [12] show that the T_i in Alcator C-Mod's ECDC plasmas is on the order of several eV, which is consistent with our result. This indicates that there is a yet to be determined mechanism of the RF absorption that is directly heating ions, including the background He and boron ions. Possible candidates are: fast electromagnetic to slow electrostatic wave mode conversion [19] and excitation of the parametric decay instability of upper and lower hybrid waves [20, 21].

The experimentally observed ion heating is qualitatively linked to the observation that the peak boron deposition rate and the I_{sat} (~n_e) are displaced radially several cm outboard from the EC resonance location at a location consistent with the upper hybrid resonance location. Apparently, the peaked ionization and RF heating takes place at the UH resonance location, not at the EC resonance location, where one would only expect resonant electron heating. This implies that the previous C-Mod studies on core Mo source rates [4], which relied on the knowledge of radial boronization profiles before the direct QMB measurements, need to be reinterpreted: the critical radial deposition location is further out in the major radius and suggests that limiter surfaces could also play a key role as a Mo source in ICRF-heated plasma discharges.

Finally, we determined that the optimized conditions for a typical boronization procedure (with 10% B_2D_6 fraction) in Alcator C-Mod are: 0.7 Pa in-vessel neutral gas pressure in the presence of the vertical field. These conditions result in the boron deposition rates of ~0.36-0.47 $\mu g/cm^2$/min (or ~1.5-2.0 nm/min) approximately 5-10 cm away (in the outboard direction) from the EC resonance. Increasing the diborane fraction to 20% almost doubles the peak boron deposition rate, allowing to obtain boron films produced in a 10% B_2D_6 discharge in a shorter period of time. However, boronization with a 20% B_2D_6 gas mix is not a typical procedure on Alcator C-Mod. The numerical Monte Carlo simulation allows us to predict the boron deposition profile on random in-vessel surfaces, such as the limiters, the ICRF antennae surfaces, etc. Boronization experiments at the highest diborane throughput show that the ECD discharge becomes power-limited and suggest that the boron deposition rates can be increased even further,

provided more RF power is injected into the plasma. The possibility of using the second EC harmonic also remains to be investigated.

6. Acknowledgments

This work was supported by US Department of Energy award DE-FC02-99ER54512.

7. References

[1] H. Hutchinson, R. Boivin, F. Bombarda et al., Phys. Plasmas, 1, 1511 (1994).

[2] B. Lipschultz, Y. Lin, M.L. Reinke et al., Phys. Plasmas, 13, 056117 (2006).

[3] E. Marmar, Y. Lin, B. Lipshultz et al., 33rd EPS Conference on Plasma Phys., Vol. 30I, O-2.005 (2006).

[4] B. Lipschultz, D.A. Pappas, B. LaBombard et al., Nuclear Fusion, Vol. 41, No. 5 (2001) 585.

[5] Vl. Bobkov, F. Braun, R. Dux et al, JNM, 390-391 (2009) 900-903.

[6] J Winter, Plasma Phys. Control Fusion, 38 (1996) 1503-1542.

[7] H.G. Esser, V. Philipps, H.B. Reimer and P. Wienhold, Nucl. Fusion, Vol. 32, No. 2 (1992) 278.

[8] G.L. Jackson, J. Winters, T.S. Taylor et al., Phys. Rev. Lett., Vol. 67, No. 22 (1991) 3098.

[9] A. Sykes, R.J. Akers, L.C. Appel et al., Nucl. Fusion, Vol. 41, No. 10 (2001) 1423.

[10] H.Y. Wang, X.M. Wang, J.H. Wu et al., Journal of Physics: Conference Series 100 (2008) 062011.

[11] B. Lipschultz, Y. Lin, E.S. Marmar et al., JNM, 363-365 (2007) 1110-1118.

[12] R.T. Nachtrieb, B.L. LaBombard, J.L. Terry et al., JNM, 266-269 (1999) 896-900.

[13] C. Lu, J. Vac. Sci Technol., Vol. 12, No. 1, (1975) 578.

[14] T. Schwarz-Selinger, A. von Keudell, and W. Jacob J. Appl. Phys. 86 (1999) 3988.

[15] C.H. Skinner, H. Kugel, A.L. Roquemore et al., JNM, 337-339 (2005) 129-133.

[16] F.F. Chen, Introduction to Plasma Physics and Controlled Fusion, Vol. 1, 2nd Ed.

[17] P.C. Stangeby, The Plasma Boundary of Magnetic Fusion Devices, Ch. 3, (2000).

[18] K. Nanbu and Y. Kitatani, J. Phys. D: Appl. Phys. 28, (1995) 324-330.

[19] T.H. Stix, Phys. Rev. Lett., Vol. 15, No. 23 (1965) 878.

[20] B. Grek and M. Porkolab, Phys. Rev. Lett., Vol. 30, No. 18 (1972) 836.

[21] M. Okabayashi, K. Chen, and M. Porkolab, Phys. Rev. Lett., Vol. 31, No. 18, (1973) 1113.

8. Figure Captions

Figure 2.1: The Surface Science Station (S^3) probe head. (a) QMB1 (radially-viewing), QMB2 (poloidally-viewing), and Langmuir probe orientation in the S^3 head, relative to the magnetic field; rotation definition also shown b) the S^3 positioned at R_{probe} = 0.60 m inside Alcator C-Mod; limiter and divertor PFCs also shown.

Figure 2.2: (a) Example QMB data with the constant decrease in resonant frequency indicating constant B deposition rate (b) Monitoring of in-vessel pressure and QMB1 temperature during the data acquisition.

Figure 3.1: I_{sat} radial (R) profiles in pure helium and 10% diborane fraction ECD discharges at (a) 0.062 Pa m^3 s^{-1} and (b) 0.080 Pa m^3 s^{-1} boron atom throughput values. The locations of the outboard limiter and estimated upper hybrid (UH) resonance are shown. The lines are to guide the eye.

Figure 3.2: Radial boron deposition rate and I_{sat} profiles at 0.062 Pa m^3 s^{-1} throughput of boron atoms. The profiles are for the QMB faces oriented (a) parallel and (b) perpendicular to the magnetic field. The locations of the outboard limiter and UH resonance are shown. The lines are to guide the eye.

Figure 3.3: (a) Peak boron deposition rates as a function of the throughput of boron atoms on the QMB face perpendicular ($\perp$) to the magnetic field. (b) The ratio between the peak boron deposition rates on the surfaces $\perp$ and // to the magnetic field as a function of the throughput of boron atoms. The lines are to guide the eye.

Figure 3.4: Boron deposition rate as a function of the local ion flux (Γ_i) for (a) the QMB face // to the magnetic field and (b) the QMB face $\perp$ to the magnetic field. In this case the global throughput of boron atoms is fixed at 0.080 Pa m^3 s^{-1} and deposition rate and ion flux are measured at different radii 0.60 m $\leq R_{probe} \leq$ 1.10 m. Boron deposition rates as a function of Γ_{ion} are plotted for 5%, 10%, and 20% B^+ ion fractions with dashed lines.

Figure 4.1: Simulation of the ratio of boron deposition on surfaces perpendicular and parallel to the magnetic field as a function of the boron ion (B^+) temperature. The expected boron ion temperature for experimental conditions is shown as a shaded region [12]. The magnetic field was 0.09 T and the ion trajectories were collisionless. The line is to guide the eye.

Figure 4.2: B^+ deposition pattern as a function of the orientation of the poloidally viewing QMB (QMB2) surface; solid squares are simulation – the B^+ temperature and magnetic field were 2 eV and 0.09 T, respectively; the ion trajectories were collisionless; open squares are experimental results. The line is to guide the eye.

Figure 4.3: Effect of ion-neutral elastic collisions on the boron ion deposition pattern on the QMB surfaces as He neutral density in background is increased – solid squares are simulation and open squares are experimental results. The lines are to guide the eye.

Figure 2.1

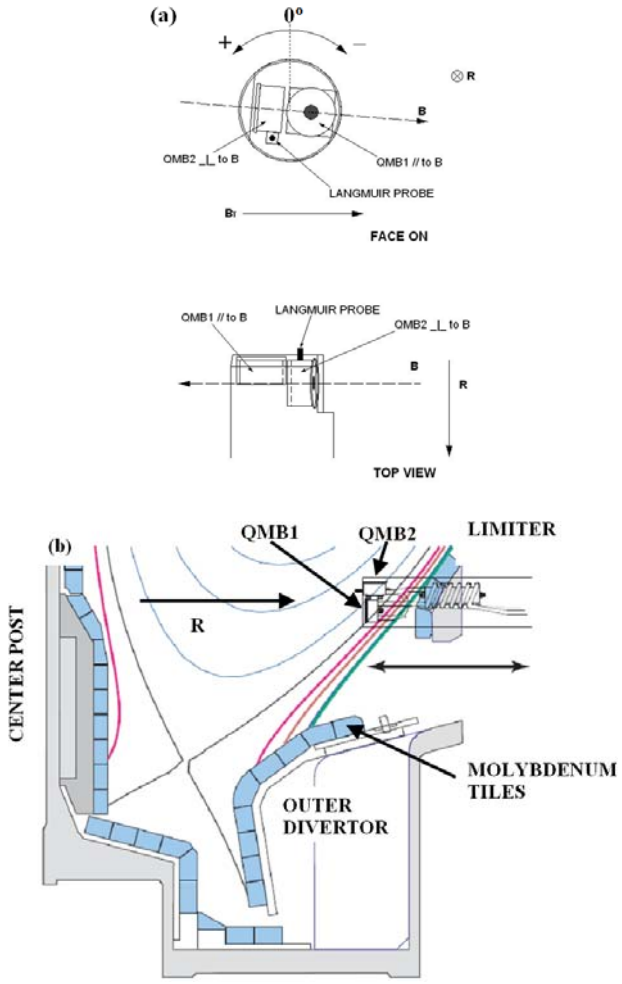
(a)
0°
+
−
⊗ R
B
QMB2 _|_ to B
QMB1 // to B
LANGMUIR PROBE
Bt
FACE ON
QMB1 // to B
LANGMUIR PROBE
QMB2 _|_ to B
B
R
TOP VIEW
(b)
QMB1
QMB2
LIMITER
R
CENTER POST
MOLYBDENUM
TILES
OUTER
DIVERTOR

Figure 2.2

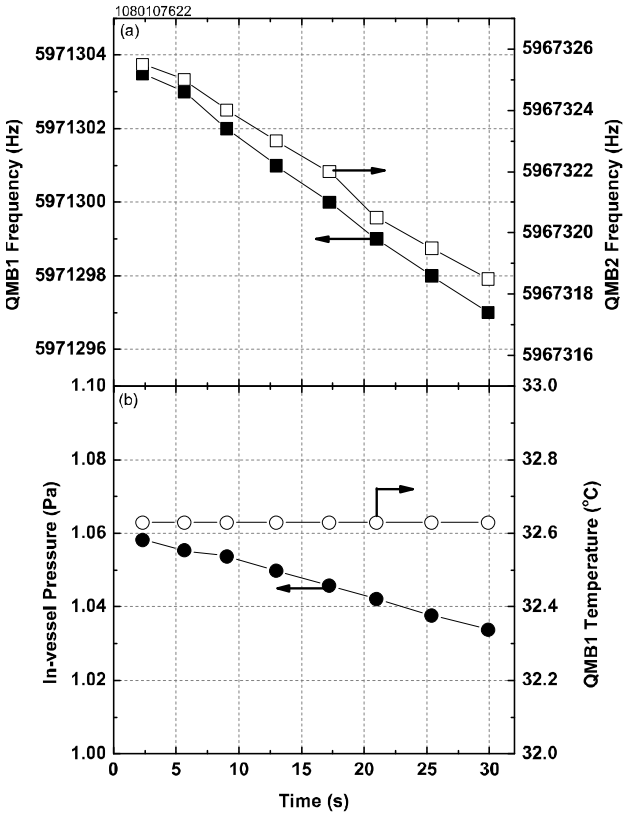
1080107622
(a)
5971304
5971302
5971300
5971298
5971296
QMB1 Frequency (Hz)
5967326
5967324
5967322
5967320
5967318
5967316
QMB2 Frequency (Hz)
(b)
1.10
1.08
1.06
1.04
1.02
1.00
In-vessel Pressure (Pa)
33.0
32.8
32.6
32.4
32.2
32.0
QMB1 Temperature (°C)
0
5
10
15
20
25
30
Time (s)

Figure 3.1

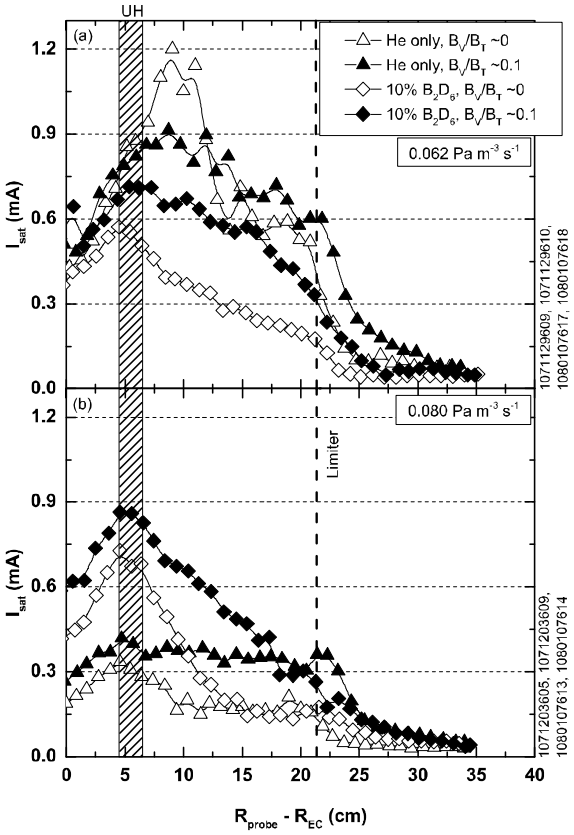
UH
(a)
He only, B_V/B_T ~0
He only, B_V/B_T ~0.1
10% B_2D_6, B_V/B_T ~0
10% B_2D_6, B_V/B_T ~0.1
0.062 Pa m^{-3} s^{-1}
1071129609, 1071129610, 1080107617, 1080107618
(b)
0.080 Pa m^{-3} s^{-1}
Limiter
1071203605, 1071203609, 1080107613, 1080107614
I_{sat} (mA)
R_{probe} - R_{EC} (cm)

Figure 3.2

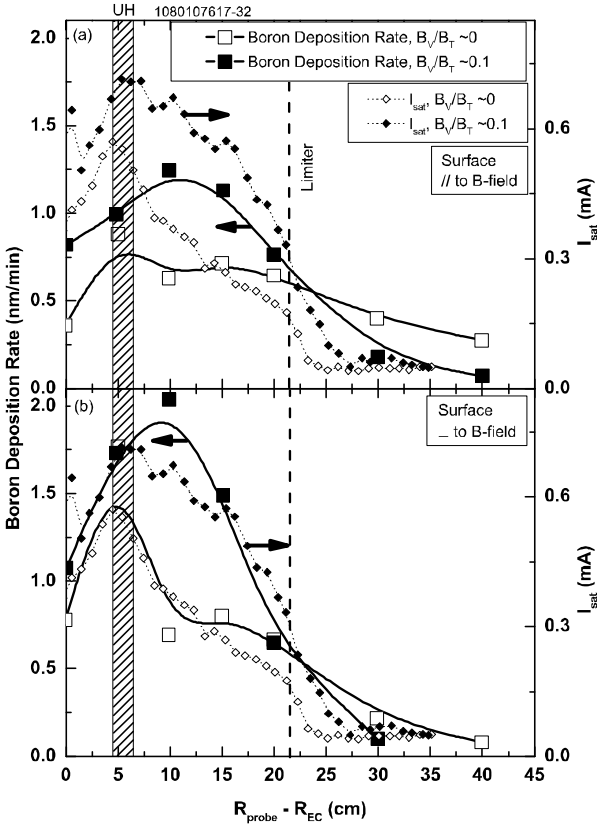
UH
1080107617-32
(a)
Boron Deposition Rate, B_V/B_T ~0
Boron Deposition Rate, B_V/B_T ~0.1
I_{sat}, B_V/B_T ~0
I_{sat}, B_V/B_T ~0.1
Surface // to B-field
Limiter
(b)
Surface _ to B-field
Boron Deposition Rate (nm/min)
I_{sat} (mA)
R_{probe} - R_{EC} (cm)

Figure 3.3

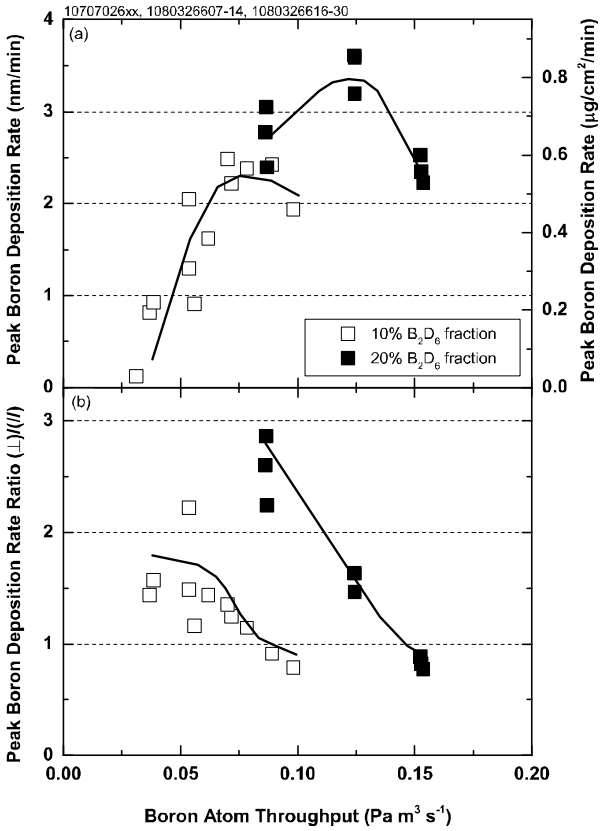
10707026xx, 1080326607-14, 1080326616-30
(a)
(b)
Peak Boron Deposition Rate (nm/min)
Peak Boron Deposition Rate (μg/cm²/min)
Peak Boron Deposition Rate Ratio (⊥)/(//)
10% B2D6 fraction
20% B2D6 fraction
Boron Atom Throughput (Pa m³ s⁻¹)
0.00
0.05
0.10
0.15
0.20

Figure 3.4

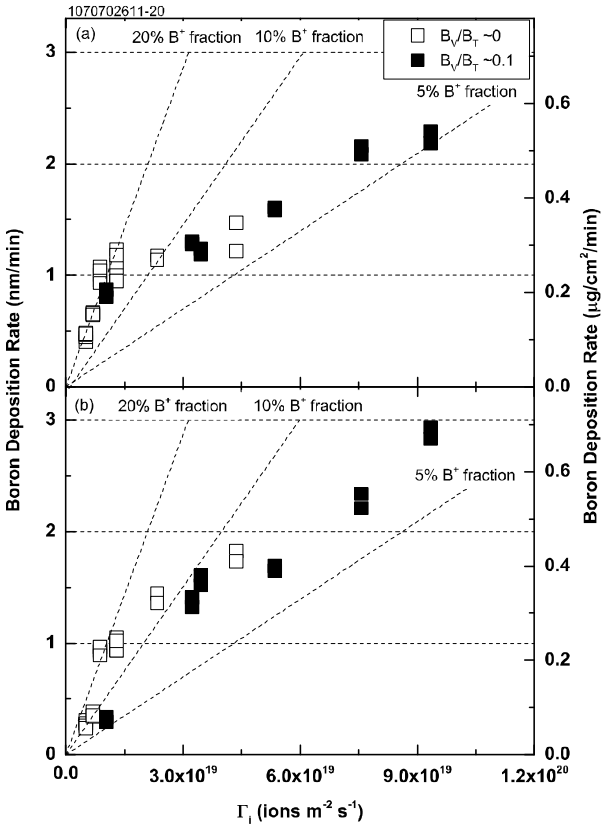
1070702611-20
(a)
20% B+ fraction
10% B+ fraction
5% B+ fraction
BV/BT ~0
BV/BT ~0.1
(b)
20% B+ fraction
10% B+ fraction
5% B+ fraction
Boron Deposition Rate (nm/min)
Boron Deposition Rate (μg/cm2/min)
ΓI (ions m-2 s-1)
0.0
3.0x10^19
6.0x10^19
9.0x10^19
1.2x10^20

Figure 4.1

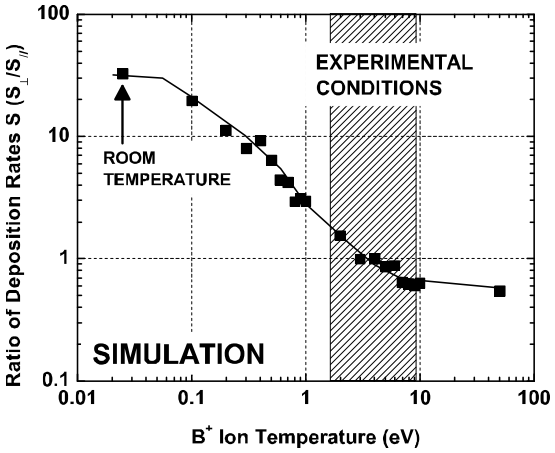
100
10
1
0.1
0.01
0.1
1
10
100
Ratio of Deposition Rates S (S⊥/S//)
B+ Ion Temperature (eV)
EXPERIMENTAL
CONDITIONS
ROOM
TEMPERATURE
SIMULATION

Figure 4.2

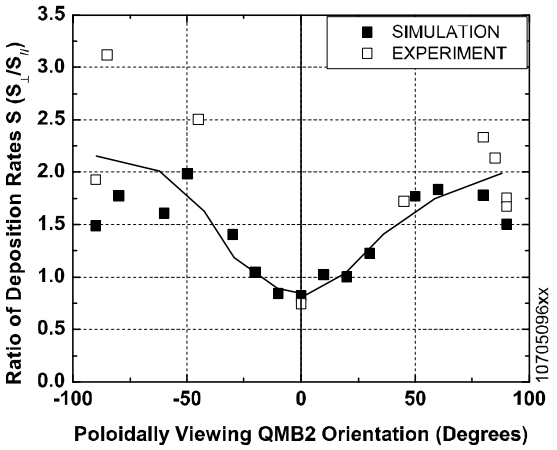
SIMULATION
EXPERIMENT
Ratio of Deposition Rates S (S⊥/S//)
Poloidally Viewing QMB2 Orientation (Degrees)
3.5
3.0
2.5
2.0
1.5
1.0
0.5
0.0
-100
-50
0
50
100
10705096xx

Figure 4.3

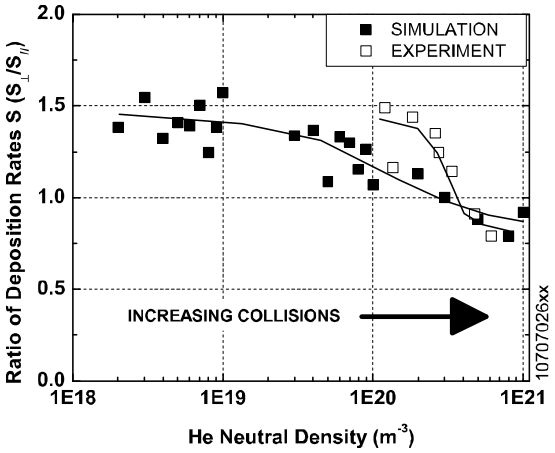
SIMULATION
EXPERIMENT
INCREASING COLLISIONS
Ratio of Deposition Rates S (S⊥/S//)
He Neutral Density (m-3)
2.0
1.5
1.0
0.5
0.0
1E18
1E19
1E20
1E21
10707026xx